Acousto-plasmofluidics: Acoustic modulation of surface plasmon resonance in microfluidic systems

Daniel Ahmed,[1] Xiaolei Peng,[2] Adem Ozcelik,[1] Yuebing Zheng,[2,a] and Tony Jun Huang[1,a]

[1]*Department of Engineering Science and Mechanics, Department of Biomedical Engineering, The Pennsylvania State University, University Park, PA 16802 USA*

[2]*Department of Mechanical Engineering, Materials Science and Engineering Program, Texas Materials Institute, The University of Texas at Austin, Austin, TX 78712 USA*

(Received 1 July 2015; accepted 10 September 2015; published online 18 September 2015)

We acoustically modulated the localized surface plasmon resonances (LSPRs) of metal nanostructures integrated within microfluidic systems. An acoustically driven micromixing device based on bubble microstreaming quickly and homogeneously mixes multiple laminar flows of different refractive indices. The altered refractive index of the mixed fluids enables rapid modulation of the LSPRs of gold nanodisk arrays embedded within the microfluidic channel. The device features fast response for dynamic operation, and the refractive index within the channel is tailorable. With these unique features, our "acousto-plasmofluidic" device can be useful in applications such as optical switches, modulators, filters, biosensors, and lab-on-a-chip systems. [http://dx.doi.org/10.1063/1.4931641]

Localized surface plasmon resonances (LSPRs) are charge density oscillations which are confined to subwavelength conductive nanoparticles within an oscillating electromagnetic field.[1–3] Associated with LSPR are sharp spectral absorption and scattering peaks as well as strong near-field electromagnetic enhancement. LSPR can play an important role in applications such as ultrasensitive spectroscopy,[4] biosensing,[3,5–7] imaging,[8–10] nanophotonic devices,[11–16] medical diagnostics and therapy.[17,18]

Applications of LSPR require active tuning of resonance wavelength as well as high sensitivity to local refractive index changes. Nanostructures of gold and silver are common for LSPR applications, and their sizes, shapes, and morphology have been optimized for LSPR applications.[19–26] For example, for gold nanospheres of LSPR extinction between 500 and 600 nm, the central wavelength of the absorption peak may be tuned over 60 nm by varying the diameter between 10 and 100 nm.[20]

The plasmonic properties of metallic nanostructures are defined upon fabrication. This fixed definition is a hurdle when dynamically reconfigurable functionalities are needed in LSPR-based devices. One solution is to build a multiplexed analysis platform, which exploits LSPR for high-throughput laboratory and clinical settings.[3,4,8–10] Yu *et al*. designed and fabricated gold nanorod based molecular probes with aspect ratios of 1.5, 2.8, and 4.5 for multiplexed identification of cell surface markers.[27] In a similar strategy, a duplexed sensor featured patterned Ag nano-triangles of two different heights, yielding plasmon resonances at 683 and 725 nm.[10,28] In these approaches, many samples are fabricated at once by multiplexing techniques, but the fabrication is complex and is suitable only for specific specimens.

The fusion of plasmonics and microfluidics, known as plasmofluidics, has yielded lab-on-a-chip devices with the advantages of integration and reconfigurability.[29–32] These plasmofluidic devices feature precise sample delivery and analysis, small sample volumes, and high integration.[33–37]

[a]Authors to whom correspondence should be addressed. Electronic mail: zheng@austin.utexas.edu (Y.B.Z.); junhuang@psu.edu (T.J.H.)

Moreover, it offers unprecedented ability to tune the device's optical properties (including LSPRs) simply by changing fluids.

Here, we demonstrate dynamic modulation of LSPR by integrating acoustics[38–42] with plasmofluidics. We developed an acoustic-based micromixing technique: millisecond-scale mixing of two laminar streams with different refractive indices. Diffusion across the interface yields localized refractive indices and creates refractive index gradient profiles.[33,43] A change in environmental refractive index of Au nanodisks fabricated on a glass substrate is induced via acoustically driven oscillating microbubbles trapped in sidewalls of the microfluidic channel. The change can be reversed by turning the acoustic field on and off, resulting in millisecond-scale, repeatable LSPR tuning. By selective mixing of input fluids with different refractive indices, we realized tailorable, millisecond-scale modulation of the refractive index.

Figure 1(a) is a schematic of the experimental setup as well as the working principle of the acoustically driven plasmofluidic device. Gold nanodisks, each of diameter 180 nm and in arrays of period 320 nm, were fabricated on glass substrates by integrating conventional nanosphere lithography. A template formed by the self-assembly of monodisperse nanospheres on flat surfaces acts as an etching/deposition mask, with two types of reactive ion etching processes.[44,45] A single-layered, Y-shaped (two inlets and one outlet) microchannel (length: 5 mm, width: 120 μm, and height: 50 μm) was fabricated of polydimethylsiloxane (PDMS) by soft lithography and a mold-replica technique.[46] The microfluidic channel periodically featured rectangular cavities. These were activated with oxygen plasma, and were bonded to the glass substrate which supported the gold nanodisk arrays. A piezoelectric transducer (273-073, RadioShack, USA) mounted to the glass slide generated acoustic waves. Once liquid was injected into the channel, air bubbles became trapped within the cavities due to contact line pinning at the leading edge of the cavity when the channel is first filled.

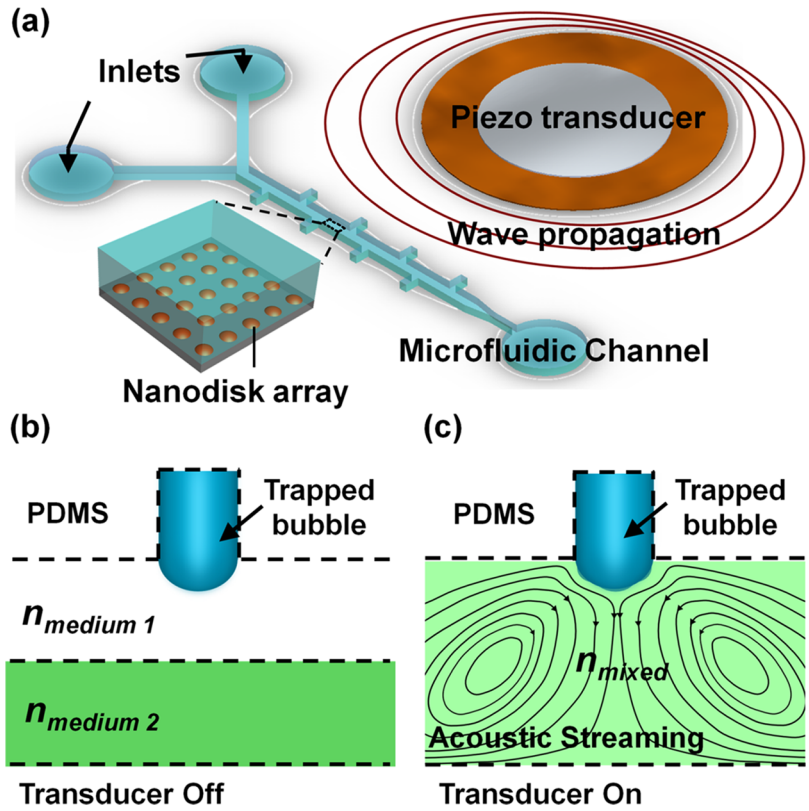

FIG. 1. (a) Schematic of the experimental setup. The microfluidic channel and the piezoelectric transducer were bonded to a glass slide with Au nanodisk arrays (Inset: Au nanodisk arrays on glass substrates). (b) Laminar flow of liquids with different refractive indices (in the absence of acoustic waves). (c) Fluid of combinatorial refractive index, resulting from mixture of two fluids actuated by acoustic waves.

When a trapped bubble was exposed to a uniform acoustic field of wavelength much larger than the bubble's diameter, the microbubble oscillated. Viscous damping in the microchannel displaced the oscillating fluid, which induced a steady flow around the air bubble, a phenomenon known as acoustic microstreaming.[47] When the frequency driven by the transducer neared the resonance frequency of the trapped microbubble, the oscillation amplitude of the liquid-air interface was maximized.[48–50] We exploited this phenomenon to realize rapid micromixing. Fig. 1(b) shows the laminar flow when the transducer was off, and Fig. 1(c) when on. The oscillating microbubbles disrupted the clear liquid-liquid interface and rapidly mixed the fluids. By regulating the fluids of different refractive indices, we modulated the LSPRs of the gold nanodisk arrays.

To demonstrate acoustic mixing, we infused the two inlets with a dye and a buffer solutions, both at 5 μL/min. Once we established a laminar flow (Fig. 2(a)), the bubbles were actuated at the resonance frequency. The developed microstreaming from the oscillating bubbles disrupted the clear liquid interface and induced mixing (Fig. 2(b)). We observed upon mixing a significant change in refractive index. Before mixing, the refractive index corresponds to the Z-profile, and the gradient at the interface depends on the flow rate and the miscibility of the two liquids (Fig. 2(c)). Once the transducer was turned on, the mixing of two fluids yielded a change in volumetric-average refractive index. With the knowledge of refractive index changes which are induced by mixing, we predicted the modulation of the LSPRs.

To demonstrate the micromixing-enabled modulation of LSPR, we used deionized water (H_2O with a refractive index of 1.33) and calcium chloride solution ($CaCl_2$ with a refractive index of 1.44

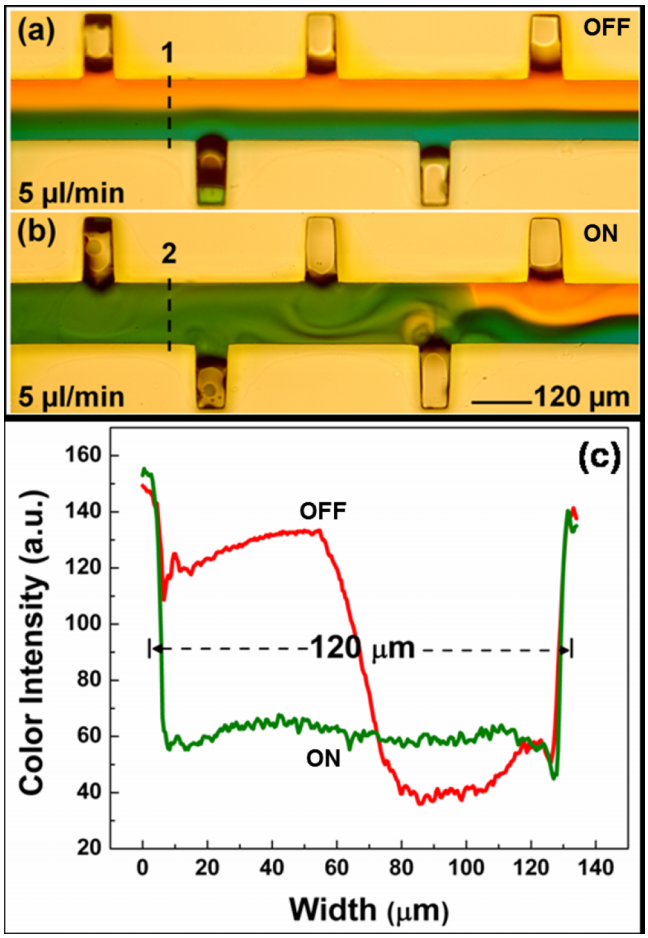

FIG. 2. (a) Laminar flow of $CaCl_2$ solution and water in the absence of acoustic waves. (b) Mixing of ink and water in the presence of acoustic waves. (c) Modulation of refractive index change across the channel with the transducer turned on and off.

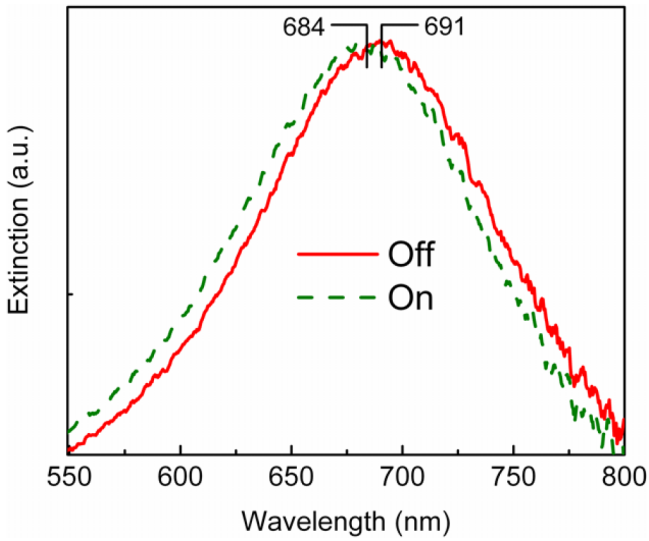

FIG. 3. Extinction spectra of the Au nanodisk arrays embedded in the microfluidic channel, both before and after switching the transducer on and off.

at a concentration of 5 M). A micro-spectroscope (Spectrapro 2300i, Acton, USA) was used before mixing to detect the signal at the $CaCl_2$ side. Figure 3 shows extinction spectra collected from the region of nanodisk array located beneath the $CaCl_2$ flow before and after switching the transducer on. The single peak arises from the in-plane dipole resonance of the Au nanodisk arrays. A blue shift occurred after mixing due to the decreased refractive index of the mixed liquid. To relate the peak shift to the micromixing-induced refractive index change, we first calibrated the sensitivity of the Au nanodisk arrays relative to the change in the surrounding refractive index. Calibration was realized by injecting liquids of known refractive indexes into the channel and recording the corresponding extinction spectra. Plotting the peak wavelength as a function of the refractive index of surrounding fluid, we found sensitivity as 120 nm/RIU (RIU: refractive index unit). Second, we calculated the refractive index before and after mixing as 1.44 (5 M) and 1.384 (2.5 M), respectively. The latter comes from the diluted $CaCl_2$ by assuming that the two flows are of the same volume and are homogeneously mixed. From Fig. 3, we measured the peak wavelength of the LSPR to be 691 nm and 684 nm before and after mixing, respectively. According to the two data pairs (refractive index: 1.44 and peak wavelength: 691; and refractive index: 1.384 and peak wavelength: 684), we calculated the ratio of the shift in peak wavelength to the change in the refractive index as 125 nm/RIU. The good matching (deviance < 5%) between the calibrated sensitivity (120 nm/RIU) and the calculated ratio (125 nm/RIU) indicates well-controlled, predictable modulations of the refractive indices, thereby indicating modulation of LSPR.

Next we calibrated the response speed. Reversible tuning of the LSPRs was achieved by switching the transducer on and off (Fig. 4). From the close-ups of the parts of the curve (Figs. 4(b) and 4(c)), the response times for the "off" and "on" switching processes were estimated to be 270 ms and 250 ms, respectively. We employed a UV-Vis-IR spectrometer (USB4000, Ocean Optics, USA) to measure the dynamic process. There is an intrinsic signal delay associated with the integration process in the photodetector. The actual response time should be faster than what was measured, and a more-accurate measurement technique based on photodiodes is under development.

In summary, we have modulated the LSPR of metallic nanostructures by acoustically-driven oscillations of sidewall-trapped microbubbles. Our work demonstrates that fluids within microchannels are effective active media for modulating LSPR, by means of efficient acoustic transduction. The modulation range and the spectra bands are flexible, and the response time is on the order of milliseconds. Our hybridized acoustic-microfluidic-plasmonic devices can lead to the development of many reconfigurable optical components such as switches and modulators.

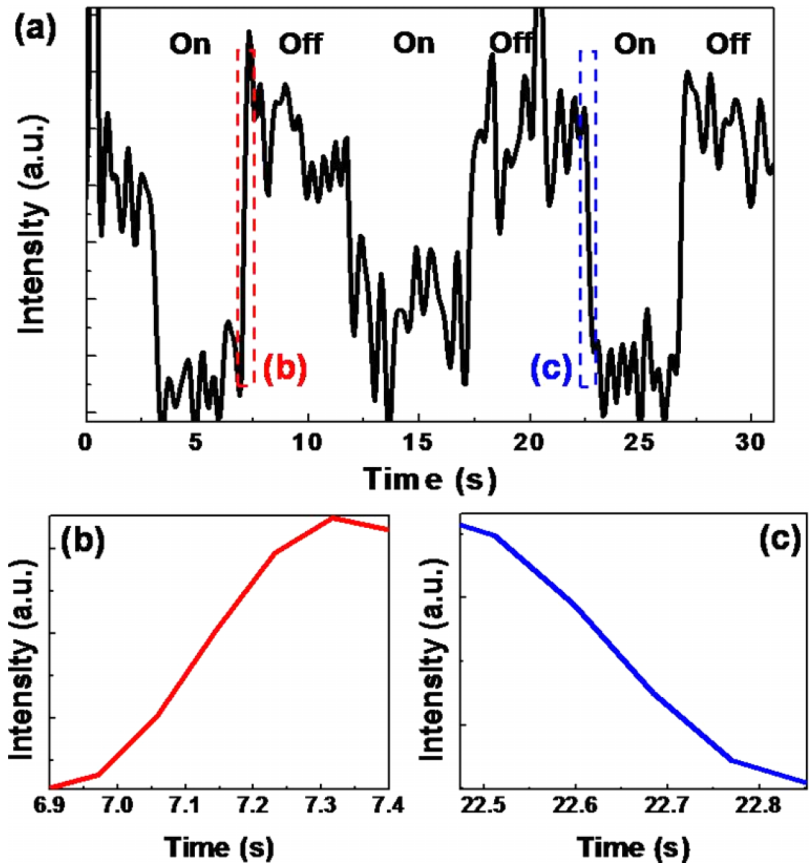

FIG. 4. (a) Time dependence of extinction efficiency for Au nanodisks embedded in the fluids when the transducer was turned on and off. (b,c) Close-ups of parts of the curve shown in (a).

ACKNOWLEDGEMENTS

We gratefully acknowledge financial support from National Science Foundation (IDBR-1455658 and CBET-1438126), National Institutes of Health (1 R01 GM112048-01A1 and 1R33EB019785-01), and the Penn State Center for Nanoscale Science (MRSEC) under grant DMR-1420620. Components of this work were conducted at the Pennsylvania State University node of the NSF-funded National Nanotechnology Infrastructure Network. Y. B. Z. recognizes support from Beckman Young Investigator Program.

[1] S.A. Maier, *Plasmonics: Fundamentals and Applications* (Springer Science & Business Media, 2007).
[2] E. Hutter and J.H. Fendler, Adv. Mater. **16**, 1685 (2004).
[3] E. Petryayeva and U.J. Krull, Anal. Chim. Acta **706**, 8 (2011).
[4] K.A. Willets and R.P. Van Duyne, Annu. Rev. Phys. Chem. **58**, 267 (2007).
[5] C. Escobedo, S. Vincent, A.I.K. Choudhury, J. Campbell, A.G. Brolo, D. Sinton, and R. Gordon, J. Micromechanics Microengineering **21**, 115001 (2011).
[6] C. Escobedo, A.G. Brolo, R. Gordon, and D. Sinton, Nano Lett. **12**, 1592 (2012).
[7] Y.B. Zheng, B. Kiraly, P.S. Weiss, and T.J. Huang, Nanomedicine **7**, 751 (2012).
[8] B. Sepúlveda, P.C. Angelomé, L.M. Lechuga, and L.M. Liz-Marzán, Nano Today **4**, 244 (2009).
[9] T. Chung, S.Y. Lee, E.Y. Song, H. Chun, and B. Lee, Sensors **11**, 10907 (2011).
[10] K.M. Mayer and J.H. Hafner, Chem. Rev. **111**, 3828 (2011).
[11] W.L. Barnes, A. Dereux, and T.W. Ebbesen, Nature **424**, 824 (2003).
[12] A. V. Zayats, I.I. Smolyaninov, and A.A. Maradudin, Phys. Rep. **408**, 131 (2005).
[13] Y. Liu, H. Zhai, F. Guo, N. Huang, W. Sun, C. Bu, T. Peng, J. Yuan, and X. Zhao, Nanoscale **4**, 6863 (2012).
[14] B. Liu, Y. Liu, and S. Shen, Phys. Rev. B **90**, 195411 (2014).
[15] Y. Zhao, S.-C.S. Lin, A.A. Nawaz, B. Kiraly, Q. Hao, Y. Liu, and T.J. Huang, Opt. Express **18**, 23458 (2010).
[16] G. Si, Y. Zhao, H. Liu, S. Teo, M. Zhang, T. Jun Huang, A.J. Danner, and J. Teng, Appl. Phys. Lett. **99**, 033105 (2011).
[17] A.J. Haes, W.P. Hall, L. Chang, W.L. Klein, and R.P. Van Duyne, Nano Lett. **4**, 1029 (2004).

[18] C. Loo, A. Lowery, N. Halas, J. West, and R. Drezek, Nano Lett. **5**, 709 (2005).
[19] C.M. Cobley, J. Chen, E.C. Cho, L. V Wang, and Y. Xia, Chem. Soc. Rev. **40**, 44 (2011).
[20] S. Link, S. Link, M.A. El-Sayed, and M. El-Sayed, J. Phys. Chem. B **103**, 8410 (1999).
[21] J.J. Mock, M. Barbic, D.R. Smith, D.A. Schultz, and S. Schultz, J. Chem. Phys. **116**, 6755 (2002).
[22] C.J. Murphy, T.K. Sau, A.M. Gole, C.J. Orendorff, J. Gao, L. Gou, S.E. Hunyadi, and T. Li, J. Phys. Chem. B **109**, 13857 (2005).
[23] N. Halas, MRS Bull. **30**, 362 (2005).
[24] S.E. Skrabalak, J. Chen, Y. Sun, X. Lu, L. Au, C.M. Cobley, and Y. Xia, Acc. Chem. Res. **41**, 1587 (2008).
[25] Z. Liu, J.M. Steele, W. Srituravanich, Y. Pikus, C. Sun, and X. Zhang, Nano Lett. **5**, 1726 (2005).
[26] J.L. Ponsetto, F. Wei, and Z. Liu, Nanoscale **6**, 5807 (2014).
[27] C. Yu, H. Nakshatri, and J. Irudayaraj, Nano Lett. **7**, 2300 (2007).
[28] C.R. Yonzon, E. Jeoung, S. Zou, G.C. Schatz, M. Mrksich, and R.P. Van Duyne, J. Am. Chem. Soc. **126**, 12669 (2004).
[29] D. Psaltis, S.R. Quake, and C. Yang, Nature **442**, 381 (2006).
[30] F.B. Myers and L.P. Lee, Lab Chip **8**, 2015 (2008).
[31] J. Kim, Lab Chip **12**, 3611 (2012).
[32] M.L. Sin, J. Gao, J.C. Liao, and P. Wong, J. Biol. Eng. **5**, 6 (2011).
[33] J. Atencia and D.J. Beebe, Nature **437**, 648 (2005).
[34] C. Rivet, H. Lee, A. Hirsch, S. Hamilton, and H. Lu, Chem. Eng. Sci. **66**, 1490 (2011).
[35] H.A. Stone, A.D. Stroock, and A. Ajdari, Annu. Rev. Fluid Mech. **36**, 381 (2004).
[36] P. Domachuk, M. Cronin-Golomb, B. Eggleton, S. Mutzenich, G. Rosengarten, and A. Mitchell, Opt. Express **13**, 7265 (2005).
[37] K. Campbell, A. Groisman, U. Levy, L. Pang, S. Mookherjea, D. Psaltis, and Y. Fainman, Appl. Phys. Lett. **85**, 6119 (2004).
[38] A. Ozcelik, D. Ahmed, Y. Xie, N. Nama, Z. Qu, A.A. Nawaz, and T.J. Huang, Anal. Chem. **86**, 5083 (2014).
[39] D. Ahmed, C.Y. Chan, S.-C.S. Lin, H.S. Muddana, N. Nama, S.J. Benkovic, and T.J. Huang, Lab Chip **13**, 328 (2013).
[40] Q. Zeng, F. Guo, L. Yao, H.W. Zhu, L. Zheng, Z.X. Guo, W. Liu, Y. Chen, S.S. Guo, and X.Z. Zhao, Sensors Actuators B Chem. **160**, 1552 (2011).
[41] P. Rogers, I. Gralinski, C. Galtry, and A. Neild, Microfluid. Nanofluidics **14**, 469 (2012).
[42] P. Agrawal, P.S. Gandhi, and A. Neild, J. Appl. Phys. **114**, 114904 (2013).
[43] A. Groisman, M. Enzelberger, and S.R. Quake, Science **300**, 955 (2003).
[44] Y.B. Zheng, B.K. Juluri, X. Mao, T.R. Walker, and T.J. Huang, J. Appl. Phys. **103** (2008).
[45] J.C. Hulteen, D.A. Treichel, M.T. Smith, M.L. Duval, T.R. Jensen, and R.P. Van Duyne, J. Phys. Chem. B **103**, 3854 (1999).
[46] Y. Xia and G.M. Whitesides, Annu. Rev. Mater. Sci. **28**, 153 (1998).
[47] W.L. Nyborg, J. Acoust. Soc. Am. **30**, 329 (1958).
[48] R.H. Liu, J. Yang, M.Z. Pindera, M. Athavale, and P. Grodzinski, Lab Chip **2**, 151 (2002).
[49] J. Feng, J. Yuan, and S.K. Cho, Lab Chip **15**, 1554 (2015).
[50] K. Ryu, S.K. Chung, and S.K. Cho, J. Assoc. Lab. Autom. **15**, 163 (2010).